

# Mathematical Modeling Of The Hydrodynamic Forces On A Low Aspect-ratio Curved Otter Board

X RAO<sup>1,2</sup>, H L HUANG<sup>1,2\*</sup>, J L Yang<sup>1,2</sup>, L Z LI<sup>1,2</sup> and S Chen<sup>1,2</sup>

<sup>1</sup>Key Laboratory of Oceanic and Polar Fisheries, Ministry of Agriculture; East China Sea Fisheries Research Institute, Chinese Academy of Fishery Sciences, Shanghai 200090

<sup>2</sup>Engineering Technology Research Center of Marine Fishing, Chinese Academy of Fishery Sciences, Shanghai 200090, China

Corresponding author's e-mail address: ecshhl@163.com

**Abstract.** As an important accessory of single trawl, otter board has the effect of providing net horizontal expansion. Hydrodynamic performance of otter board directly affects net horizontal expansion, affects further the catching and fishing efficiency<sup>[1-2]</sup>. For improving the fishing efficiency and technology level and solving the world energy crisis in some way, carrying out the research of trawl door hydrodynamic performance in order to design and optimize new energy-efficient with high expansion and low drag force otter board becomes a new researchers' focus<sup>[2]</sup>. This paper selects a low aspect-ratio curved otter board as research object, presents a method based on the flume experiment results and for mathematical modeling of the hydrodynamic forces on the otter board. These forces have been found as a function of angles of attack and slip. The coefficients are parameterized for smoothing and computational performance. A method is summarized for extending to the evaluation of arbitrary shape otter board and outside the normal operating. A verified by experiment results computational efficient model of the steady state hydrodynamic forces is finally proposed, suitable for trawl control system design and analysis.

## 1. Introduction

As an important and traditional marine fishing method, trawl fishing also faces a challenge. In order to continue playing important role in marine fishing, promote the sustainable development of trawl fishing, solve the world energy crisis, the development of fishing gear is certainly necessary. As an important accessory of single trawl, otter board has the effect of providing net horizontal expansion. Hydrodynamic performance of the otter board directly affects net horizontal expansion, affects further the catching and fishing efficiency<sup>[1-2]</sup>.

It is assumed to be significant to study on hydrodynamic performance of the otter board from both economic and environmental reasons. It is also an important development direction of the fishery engineering in our country now and future.

Since 1970s, with the development of single trawl fishing, some advanced fishing countries have begun to pay attention to the research on hydrodynamic performance of otter board. The hydrodynamic performance of various otter boards was evaluated based on the wind tunnel and flume experiment, a series of otter boards with better performance and stability were developed.

Matsuda carried out flume experiment on V type otter board, the relationship between lift drag ratio and attack angle is obtained, the attack angle of the maximum lift drag ratio was confirmed, and the



trend of lift-drag ratio inside normal operation was analyzed<sup>[3]</sup>. The overall evaluation of hydrodynamic performance of V-type otter board was summarized

Guan Changtao carried out wind tunnel tests on 5 kinds of high aspect ratio otter boards. The hydrodynamic performance was evaluated and compared with lift force, drag force, lift-drag ratio and moment coefficients. Otter board with best performance was selected as the basic model, new modified otter board was designed and produced<sup>[4]</sup>.

A biplane-type otter board composed of a pair of ordinary cambered otter boards with the same size and shape was proposed by Fukuda, a series of flume experiments was carried out using 1:10 scale models. Lift force, drag force, lift-drag ratio and moment coefficients were measured with a three component balance at attack angles ranging from 0-70°. Investigated and compared with ordinary types, the maximum lift coefficient of a biplane type was nearly the same and the range of the attack angle was wider with higher lift force than ordinary type. This suggested that the former is hydrodynamically more efficient<sup>[5-6]</sup>.

An improved otter board used with semi-pelagic trawl net was evaluated and compared the lift and drag characteristics with conventional one used in Ise-wan Bay. It indicated that the drag coefficient of improved one was smaller, lift-drag ratio was higher, even the otter board distance was 1.1-1.2 times wider<sup>[7]</sup>.

To analysis the hydrodynamic performance of low aspect ratio vertical cambered otter board under different angle of attack, the drag and lift coefficient of model otter board was measured and calculated through flume experiment. The results showed the trend of coefficient versus angle of attack. By comparing the hydrodynamic performance of different types of otter boards, provide a reference basis for the rational use and further development of the new types of otter board<sup>[8]</sup>.

With the maturation of the flume and wind tunnel experiment, the numerical simulation method was introduced by scholars, the development and accuracy of the hydrodynamic performance evaluation were intended to be promoted.

Li Chongcong carried out both the flume experiment and numerical simulation on the V type otter board used near the Qingdao coast. FLUENT was used to calculate the flow regime of various depth sections. The lift, drag coefficient, lift-drag ratio, and best operation attack angle were obtained. The relative error between the numerical simulation and the test was about 15%<sup>[9]</sup>.

A method for mathematical modeling of the hydrodynamic forces on the trawl doors were presented. These forces were divided into six dof steady-state forces and transient effects. Hydrodynamic coefficients have been measured as a function of attack and slip angles. The model was extended to arbitrary otter board shape. The transient effects are described as functions of relative accelerations between the trawl door and the ambient water, angular velocities of the trawl door and circulation buildup. The proposed computational model was suitable for trawl control system design and analysis<sup>[10]</sup>.

Various structural parameters of otter board were selected to conducted numerical simulation to form the optimization scheme, the difference of the coefficients results were discussed and the final optimization design which increased the lift-drag ratio by 10% was obtained<sup>[11-12]</sup>.

It can be found as, the research trend and point have been transferred from the experimental study to the numerical simulation. Compared with wind tunnel or flume experiment, numerical simulation takes shorter time and less labor, it would be a very important direction with urgent need.

But the existing numerical simulation research was lack of accuracy, so improved and optimized model with high accuracy need to be developed and expanded to wider application.

In this paper, a low aspect-ratio curved otter board suitable for semi-pelagic trawl net in low speed operation is selected as the research object. Based on the flume experiment data, the mathematical model is established and extended to the arbitrary shapes and outside the normal operation, and the accuracy is proved.

## 2. Material and Method

### 2.1. Flume experiment setup

The experiment was conducted in the recirculating water tank of the East China Sea Fisheries Research Institute. The scale of the experimental section is 180cm \* 50cm \* 50cm and the maximum flow velocity is 2.5m/s. The otter board model was located in the middle section of the flume, and connected with the three component force sensor. The sensor was fixed on the rotary table of the machine tool. By adjusting the rotary table, the angle of attack angle could be changed. The experiment setup is shown in Fig 1. The measuring instrument is LSM-B-500NSA1-P three component force sensor manufactured by the Japan electric power company. The measuring range is 500N, and the measuring data are recorded by computer.

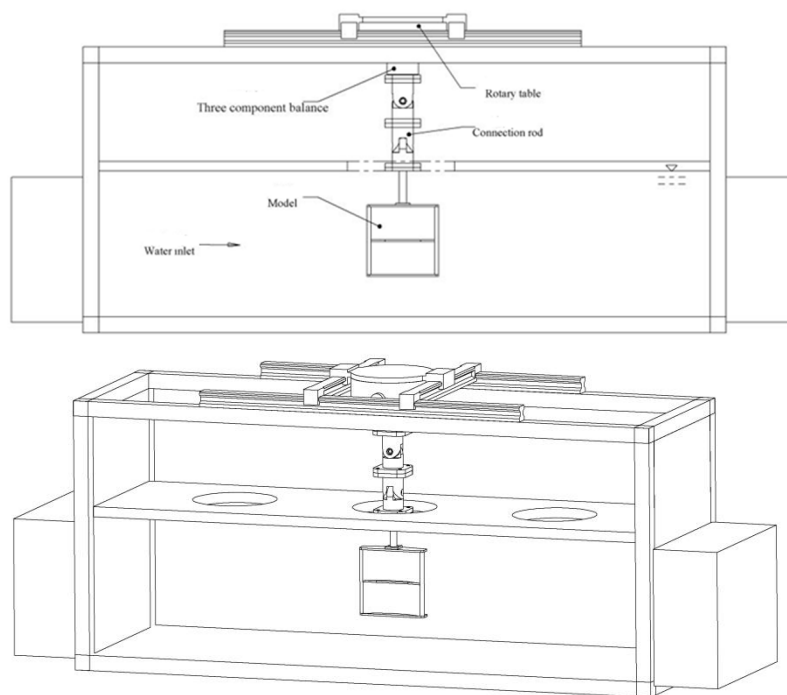


Figure 1. Flume experiment setup

### 2.2 otter board model

According to the similarity principle of fluid mechanics, the Reynolds similarity rule is adopted, the Reynolds number of the otter board model equals to the object. The model is made of stainless steel with a thickness of 2mm.

The cross-section sketch map is outlined in Fig 2. The aspect ratio of this otter board is defined as 1.0, where chord length is 20cm and the area is 0.04 m<sup>2</sup>. The model is in scale of 1:5, other structural parameters are shown as Tab 1.

Tab 1. Otter board model structural parameters

| Model           | Foil deflection         | scale | chord length (cm) | Aspect ratio | Area(m <sup>2</sup> ) |
|-----------------|-------------------------|-------|-------------------|--------------|-----------------------|
| Vertical curved | 15%(inside);8%(outside) | 1: 5  | 20                | 1.0          | 0.04                  |

### 2.3 Experimental conditions

The experimental velocity range is 20cm/s-120cm/s. In the experiment, when the flow velocity is greater than a certain value, the hydrodynamic coefficients basically keep almost stable called

automatic model region. The hydrodynamic coefficients discussed in this paper are measured and taken the average value in the region. Fig 3. shows the combinations of angles for the recorded measurements, the measurement points were primarily set to give high precision in the normal operation range. To provide the possibility of interpolation outside the normal operation, measurements for extreme orientations were also recorded.

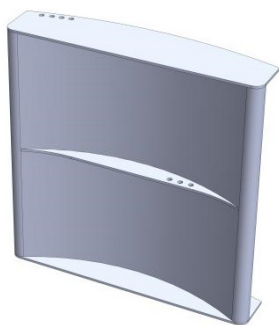


Figure 2. Sketch map of otter board model

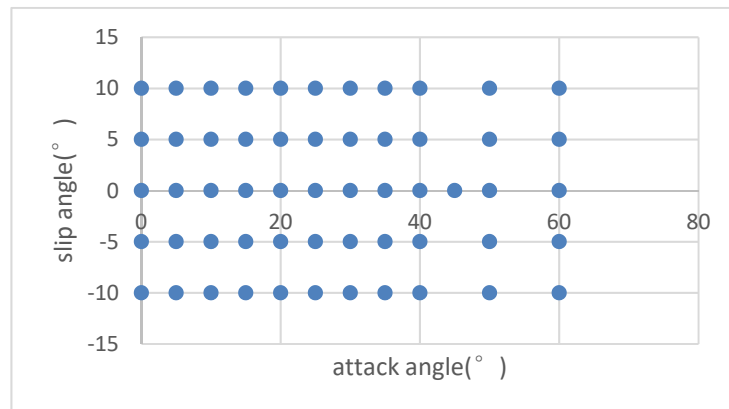


Figure 3. The setup combination of angles for the recorded measurements

### 3. Otter board hydrodynamic properties results

#### 3.1 Flume experiment results

The measured steady-state hydrodynamic force coefficients are shown in Figs 4–6, the hydrodynamic steady state force coefficients are found as<sup>[10]</sup>:

$$C_{r,i}(\alpha, \beta) = \frac{f_{r,i}(\alpha, \beta)}{0.5\rho_w A_m U_m^2}, i=1,2,3 \quad (1)$$

Where  $\alpha$  is attack angle,  $\beta$  is slip angle,  $\rho_w$  is the water density,  $A_m$  is the plan-form area,  $U_m$  is the flow velocity, subscript m means model.

$$C_L(\alpha, \beta) = \frac{(f_{r,1}(\alpha, \beta) \cos \beta + f_{r,3}(\alpha, \beta) \sin \beta) \cdot \cos \alpha + \sin \alpha f_{r,2}(\alpha, \beta)}{0.5\rho_w A_m U_m^2} \quad (2)$$

$$C_D(\alpha, \beta) = \frac{(f_{r,1}(\alpha, \beta) \cos \beta + f_{r,3}(\alpha, \beta) \sin \beta) \cdot \sin \alpha + \cos \alpha f_{r,2}(\alpha, \beta)}{0.5\rho_w A_m U_m^2} \quad (3)$$

$$C_S(\alpha, \beta) = \frac{f_{r,1}(\alpha, \beta) \sin \beta - f_{r,3}(\alpha, \beta) \cos \beta}{0.5\rho_w A_m U_m^2} \quad (4)$$

The measured steady-state hydrodynamic force coefficients (lift, drag and shear) are shown in Figs 7–9, according to equation (2)–(4)<sup>[12]</sup>.

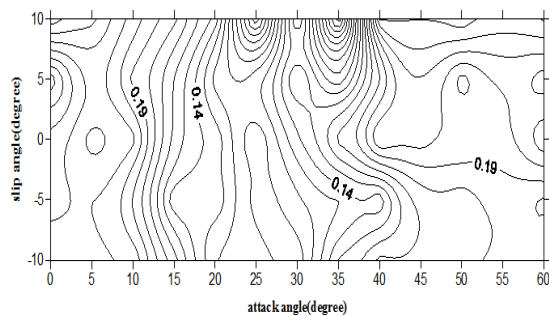


Figure 4. Measured coefficient of hydrodynamic forces  $C_{r,1}$  for varying angles of slip and attack

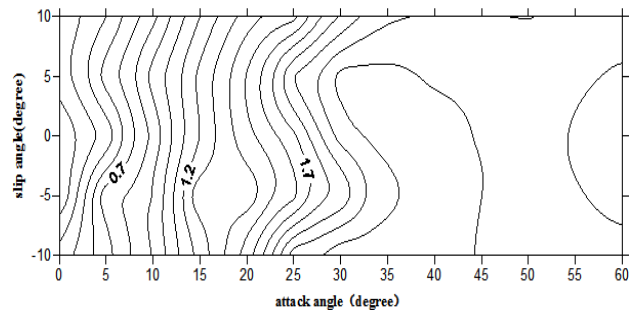


Figure 5. Measured coefficient of hydrodynamic forces  $C_{r,2}$  for varying angles of slip and attack

Fig 4. shows the coefficients of hydrodynamic force about the x-axis of sensor for different hydrodynamic orientation angles of the model. For a given attack angle in the region of  $5^\circ$ - $45^\circ$ , there seems to be a symmetric relationship between coefficient and attack angle, the minimum value appears at that attack angle approximately equals to  $25^\circ$ . Also a symmetric relationship between coefficient and slip angle while attack angle is in the region of  $10^\circ$ - $25^\circ$ .

Fig 5. shows the coefficient of hydrodynamic force about the y-axis for different hydrodynamic orientation angles of the model. For attack angle between  $0^\circ$ - $30^\circ$ , the coefficient seems to increase roughly proportional to the angular distance, slip angle seems almost no influence to efficient while attack angle is in the region of  $10^\circ$ - $25^\circ$ .

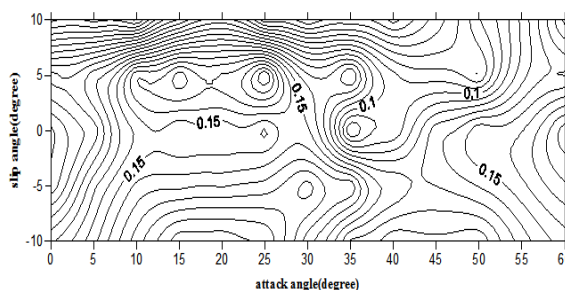


Figure 6. Measured coefficient of hydrodynamic forces  $C_{r,3}$  for varying angles of slip and attack

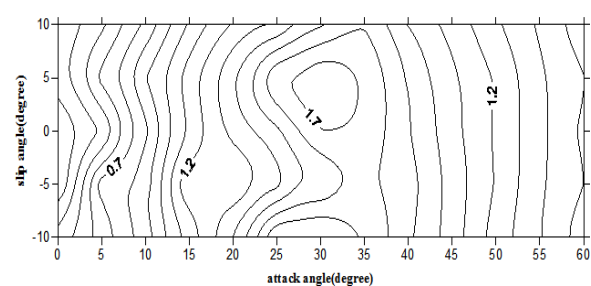


Figure 7. Measured lift force coefficient  $C_L$  for varying angles of slip and attack

Fig 6. shows the coefficient of hydrodynamic force about the z-axis for different hydrodynamic orientation angles of the model. For attack angle between  $0^\circ$ - $60^\circ$ , the coefficient seems a symmetric relationship between coefficient and attack angle, the maximum value appears at that attack angle approximately equals to  $25^\circ$ .

Fig 7. shows the lift force coefficient of the model for different hydrodynamic orientation angles. The slip angle has small influence on lift force coefficient with attack angle up to  $15^\circ$  and fairly no impact with attack angle greater than  $35^\circ$ . Lift force coefficient increases approximately linearly at the first with the attack angle increasing, then the trend is declining and maximum value is approximately 1.809 when attack angle is  $30^\circ$  and slip angle is  $-10^\circ$ . After the appearance of maximum value, lift force coefficient then decreases linearly.

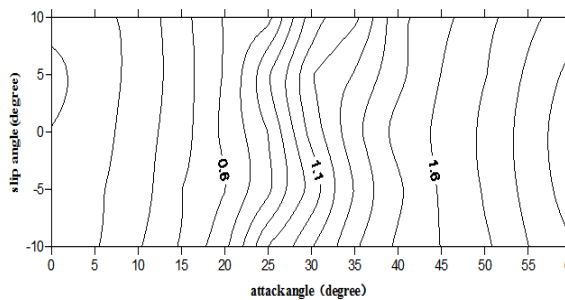


Figure 8. Measured drag force coefficient  $C_D$  for varying angles of slip and attack

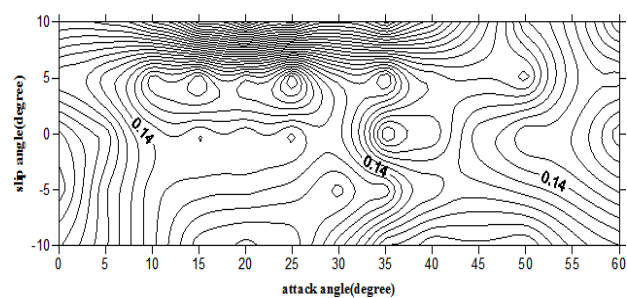


Figure 9. Measured shear force coefficient  $C_S$  for varying angles of slip and attack

Fig 8. shows drag force coefficient of the model for different hydrodynamic orientation angles. The drag coefficient is fairly independent of the slip angle, and linearly increases with attack angle. For the hydrodynamic orientation angles with maximum lift force 1.809 (attack angle = 30°, slip angle = -10°), the drag coefficient is approximately 1.196, the calculated lift-drag ratio  $k = 1.809/1.196 = 1.513$ . For the hydrodynamic orientation angles with drag force 0.332 and lift force 0.896 (attack angle = 10°, slip angle = 5°), the maximum lift-drag ratio 2.700 is obtained.

It could be seen that both the lift and drag coefficients are quite indifferent to changes of slip angle during normal operation. It is very important to operation control, means not too much attention need to be paid to slip angle adjusting.

Fig 9. shows the coefficient of hydrodynamic shear force on the model for different hydrodynamic orientation angles. The shear force seems symmetric with attack angle when slip angle is negative and out of order when slip angle is positive; it may be because of the connection rod interference.

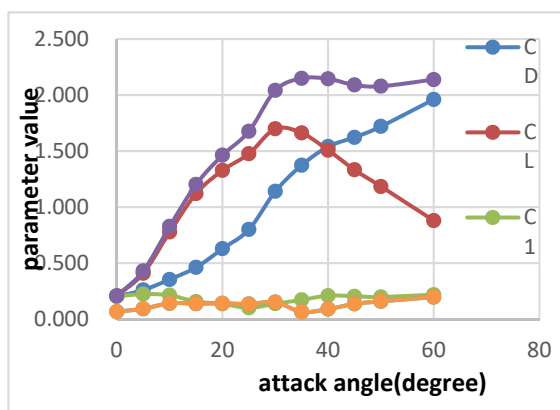


Figure 10. All coefficients value for zero slip angle

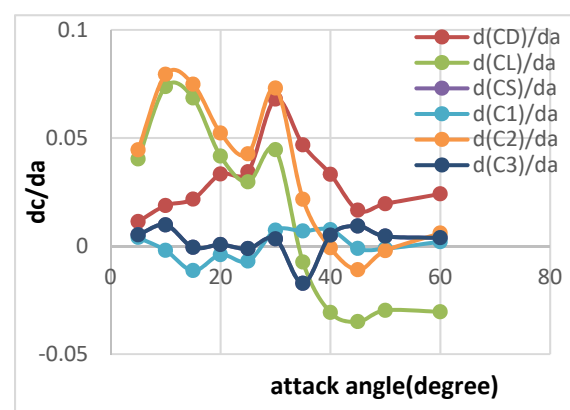


Figure 11. The derivative of coefficients with respect to angle of attack

Fig. 10 shows all coefficients for zero slip angle and its derivative with respect to attack angle is shown in Fig. 11. The lift coefficient shows a trend of increasing firstly then decreasing with the

increase of attack angle, the drag coefficient reflected an upward trend with the increase of attack angle. For the hydrodynamic orientation angles with maximum lift force 1.699(attack angle=30°), the drag coefficient is approximately 1.140, the calculated lift-drag ratio  $K = 1.699/1.140 = 1.513$ . For the hydrodynamic orientation angles with drag force 0.463 and lift force 1.120(attack angle=15°), the maximum lift-drag ratio 2.421 is obtained.

### 3.2 Parameterization of hydrodynamic Coefficients

The main purpose of the paper was to propose a mathematical model based on the flume experiment results for evaluating the otter board hydrodynamic performance.

Finding the fitting curve and formulation and making the coefficients parameterized, then the model could be used in evaluation more smoothly and accurately, even in extreme working conditions.

Rational arrangement of experiment series and the validity in the normal working area of the trawl door were emphasized to control the calculation error.

In this paper, there are 56 different combinations of orientation angles measurements for a grand total, most combinations locate in normal operation region. In the further, more extreme condition could be conducted to improve the validation.

The parameter functions  $\hat{C}_{r,in}$  return the three coefficients as a function of attack angle, slip angle, and a constant matrix  $K$ , which needs to be optimized to reflect the experimental data as well as possible.

For each dof, a candidate object function is proposed to be:

$$O_i = \hat{C}_{r,in}(\alpha_n, \beta_n, \hat{K}_{r,i}) - C_{r,in} \quad (5)$$

where  $C_{r,in}$  is the measurement  $n$  of the coefficient  $i$ ,  $\hat{C}_{r,in}$  is the calculated coefficient  $i$  for this measurement, and  $K$  is the row of constant matrix needs to be optimized.

The fitting curve function of the Matlab software, are then used in finding each row of the constant matrix that gives the lowest value of the object function of each vector.

When this matrix of 30 parameters is inserted into object functions, the steady-state coefficients in all three dof can be calculated as shown:

$$\begin{aligned} \hat{C}_{r,in}(\alpha_{in}, \beta_{in}, K_{r,in}^{opt}) &= p_{00} + p_{10}\alpha_{in} + p_{01}\beta_{in} + p_{20}(\alpha_{in})^2 \\ &+ p_{11}\alpha_{in}\beta_{in} + p_{02}(\beta_{in})^2 + p_{30}(\alpha_{in})^3 \\ &+ p_{21}(\alpha_{in})^2\beta_{in} + p_{12}(\beta_{in})^2\alpha_{in}^m + p_{03}(\beta_{in})^3 \end{aligned} \quad (6)$$

where the optimal matrix is shown as:

$$K_r^{opt} = \begin{bmatrix} 0.137 & 0.012 & 0.008 & 0.033 & 0.005 & 0.007 & -0.011 & -0.002 & -0.002 & 0.003 \\ 1.778 & 0.693 & 0.067 & -0.26 & 0.002 & -0.007 & -0.01 & 0.016 & 0.018 & -0.075 \\ 0.157 & -0.044 & -0.01 & -0.021 & 0.0075 & -0.018 & 0.031 & 0.01 & -0.003 & -0.002 \end{bmatrix} \quad (7)$$

Figs. 12 shows the parameterized coefficients and the experiment results. Based on the optimization results,  $R^2 = 0.57; 0.97; 0.70$  in proper order.



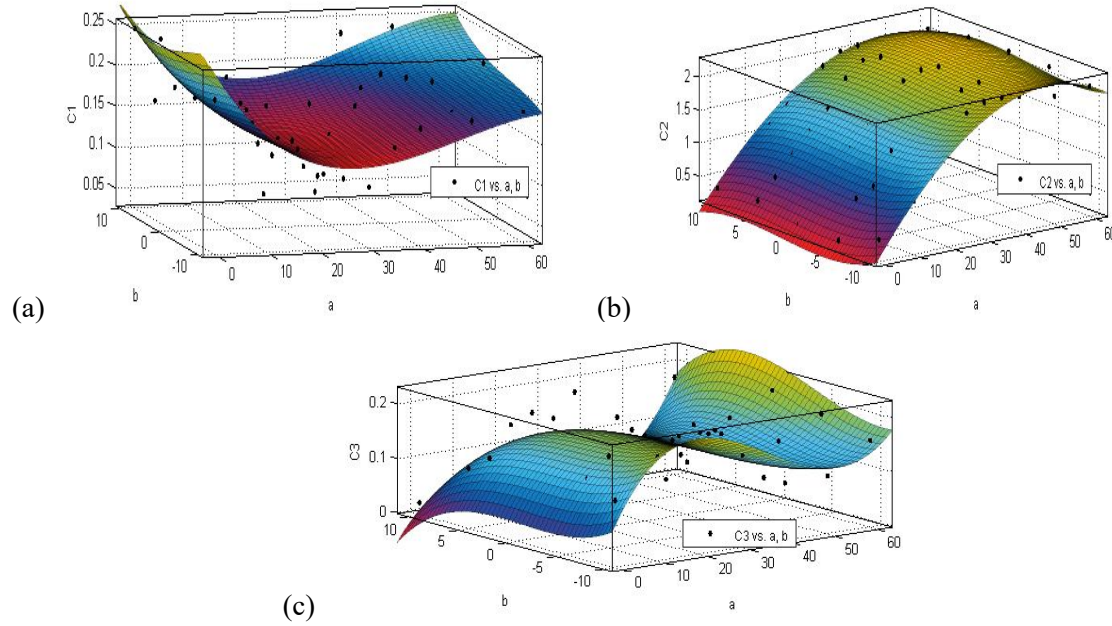


Figure 12. The comparison of parameterized coefficients and the experiment results

### 3.3 Extended mathematical model of an arbitrary otter board

Varying otter boards have different hydrodynamic properties, which need to be measured or calculated for each object. An extended mathematical model based on the model from the previous section is proposed. To ensure the validation of the estimation results, the shape and structure of otter board need to be similar without taking into account the curvature, size, placement.

The hydrodynamic parameters of the otter board as following should be obtained firstly (for zero slip angle):

- the attack angle when maximum lift is measured  $\alpha_{\max}^d$  ;
- the attack angle when no lift force is measured  $\alpha_0^d$  ;
- the maximum lift coefficient  $C_{L,\max}^d$  ;
- the drag coefficient at  $\alpha_{\max}^d, C_{D,\max}^d$  ;

Then hydrodynamic coefficients may then be approximated as:

$$\bar{C}_{dr}(\alpha^d, \beta^d) = C_{dm} \cdot \bar{C}_{mr}(\alpha^m, \beta^m) \quad (8)$$

Where, superscript d means arbitrary otter board, m means model of this paper, then :

$$\begin{aligned} \alpha^m &= \alpha_0^m + (\alpha_d + \alpha_0^d) \frac{\alpha_{\max}^m - \alpha_0^m}{\alpha_{\max}^d - \alpha_0^d} \\ \beta^m &= \beta^d \\ C_{dm} &= \text{diag} \left\{ \frac{C_{D,\max}^d}{C_{D,\max}^m}, \frac{C_{L,\max}^d}{C_{L,\max}^m}, 1 \right\} \end{aligned} \quad (9)$$

where  $\alpha_{\max}^m = 30^\circ$ ,  $\alpha_0^m = -5^\circ$ ,  $C_{D,\max}^m = 1.14$ ,  $C_{L,\max}^m = 1.699$ .

### 3.4 Hydrodynamic coefficients Outside the Normal Operation Range



Since most of experiment series were in the normal working area, error could appear outside the normal operation. Therefore, it is necessary to analyze the model cover all possible combinations of the orientation angles[10].

It is assumed that additional damping force appears and leads to the hydrodynamic coefficients reducing sharply toward zero outside normal operation range, and then otter board would return to normal operation range.

A reducing function  $r$  is proposed to describe the damping force, which equals to 1 in the normal operation, and decreases sharply to 0 outside this range:

$$r = 1 / [1 + 1.7^8 [(k_2 \alpha_{\max}^d - \alpha^d)^8 + (\beta^d - k_3)^8]] \quad (10)$$

where  $k_2 = 2/3$ ,  $k_3 = 0.17$ .

This reducing function is shown in Fig. 13 for the model used in the experiment. The hydrodynamic forces will be then calculated as:

$$\bar{\tau}_{dr,i} = 0.5 \rho_w A_d U_d^2 \bar{C}_{dr,i} r - \rho_w A_d U_d (1-r) v_{dw,i} \quad (11)$$

Where  $v_{dw}$  is angle velocity.

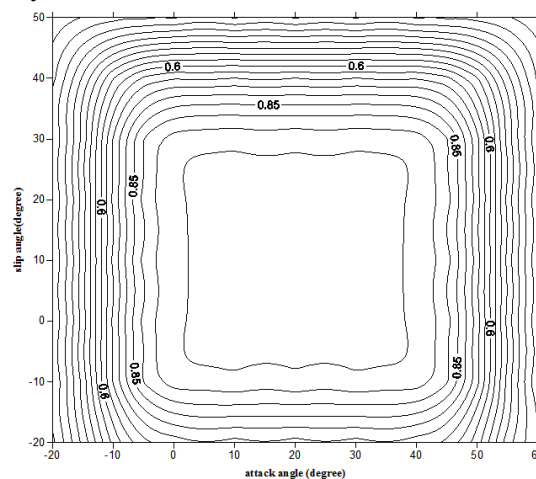


Figure 13. The value of reducing function for the experiment model

#### 4. Discussion

This paper proposed a validation model based on flume experiment for otter board hydrodynamic performance evaluation. The pity is not every coefficient has good estimation, the following research should start with reasonable arrangement of experimental series, limiting the influence of connecting rod and improve the accuracy of experiments. Extended model was also proposed for arbitrary otter board similar as vertical curved one, some models could be chosen to complete the comparison work and discuss the application range.

#### ACKNOWLEDGMENT

The authors would like to thank the support of Natural Science Foundation of China project Youth fund (31402351); Central Public-interest Scientific Institution Fundamental Research Fund (2014T01)

#### References

- [1] Xu B S, Zhang X and Wang M Y 2010 *A review on the trawl otter board evolution (Journal of Fujian Fisheries vol 3 )* no.1 pp 86-90
- [2] Zhang X, Wang M Y and Xu B S. A 2004 *Primary study on type, structure and performance of trawl otter board (Journal of Fishery Sciences of China, vol 11)* no.1 pp 107-13
- [3] Matsuda E, Hu F and Ishizawa S. 1998 *Hydrodynamic characteristics of vertical V type otter*

- board(*Bulletin of the Japanese Society of Scientific Fisheries* vol 56) no 11 pp 1815- 20
- [4] Guan C T and Pan S D 1998 *Experimental study on the selection and design of trawl doors for large pelagic trawl*(*Marine Fisheries Research* vol 19) no.2 pp 93-100
- [5] Fukuda K, Matsuda K and Hu F 1997 *A model experiment on hydrodynamic characteristics of biplane-type otter board*(*Bulletin of the Japanese Society of Scientific Fisheries* vol 63) no.2 pp 07-12
- [6] Fukuda K, Fuxiang H and Tokai T 1999 *Effects of aspect and camber ratios on hydrodynamic characteristics of biplane-type otter board.*(*Nippon Suisan Gakkaishi* vol 65) no.5 pp 860-65
- [7] Yamasaki S, Matsushita Y and Kawashima T 2007 *Evaluation of a conventional otter board used in trawl fishery in Ise-wan Bay and proposal of a new design*(*Nippon Suisan Gakkaishi*, vol 73) no.2 pp 220
- [8] Liu J and Huang H L 2013 *Hydrodynamic characteristics of low aspect ratio vertical cambered otter board*(*Journal of Fisheries of China* vol 37) no.11 pp 1742-49
- [9] Li C C 2012 *Preliminary study on the hydrodynamic performance and numerical simulation of a V-shaped otter board*(Qingdao:,Ocean University of China) Master degree Thesis
- [10] Reite K J and Sorensen A J 2006 *Mathematical modeling of the hydrodynamic forces on a trawl door*(*Oceanic Engineering* vol 31) no.2 pp 432-53
- [11] Jonsson E, Hermannsson E and Juliusson M 2013 *Computational fluid dynamic analysis and shape optimization of trawl-doors* (Grapevine, Texas)
- [12] Leifsson L, Koziel S and Jonsson E 2014 *Hydrodynamic Shape Optimization of Fishing Gear Trawl-Doors*(*Simulation and Modeling Methodologies, Technologies and Applications. Springer International Publishing*) pp 305-18